International Journal of Chemical Studies

P-ISSN: 2349–8528
E-ISSN: 2321–4902
www.chemijournal.com
IJCS 2022; 10(6): 111-124

Received: 15-09-2022
Accepted: 20-10-2022

Mougo André Tigori
Laboratoire des Sciences et Technologies de l'Environnement, UFR Environnement, Université Jean Lorougnon Guédé, BP 150 Daloa, Côte d'Ivoire

Aboudramane Koné
Laboratoire des Sciences et Technologies de l'Environnement, UFR Environnement, Université Jean Lorougnon Guédé, BP 150 Daloa, Côte d'Ivoire

Amadou Kouyaté
Laboratoire des Sciences et Technologies de l'Environnement, UFR Environnement, Université Jean Lorougnon Guédé, BP 150 Daloa, Côte d'Ivoire

Yeo Mamadou
Laboratoire de Constitution et de Réaction de la Matière, UFR SSMT, Université Félix Houphouët-Boigny, 22 BP 582 Abidjan 22, Côte d'Ivoire

Doumadé Zon
UFR des Sciences Biologiques, Université Péléforo Gon Coulibaly, Korhogo, Côte d'Ivoire

Drissa Sissouma
Laboratoire de Constitution et de Réaction de la Matière, UFR SSMT, Université Félix Houphouët-Boigny, 22 BP 582 Abidjan 22, Côte d'Ivoire

Paulin Marius Niamien
Laboratoire de Constitution et de Réaction de la Matière, UFR SSMT, Université Félix Houphouët-Boigny, 22 BP 582 Abidjan 22, Côte d'Ivoire

Corresponding Author:
Mougo André Tigori
Laboratoire des Sciences et Technologies de l'Environnement, UFR Environnement, Université Jean Lorougnon Guédé, BP 150 Daloa, Côte d'Ivoire

Adsorption and inhibitive effect of 2-(5-nitro-1H-benzimidazol-2-yl)-3-(4-methoxyphenyl) acrylonitrile on copper corrosion in 1M HNO_3

Mougo André Tigori, Aboudramane Koné, Amadou Kouyaté, Yeo Mamadou, Doumadé Zon, Drissa Sissouma and Paulin Marius Niamien

Abstract
Current study proposed to assess, the inhibition effect of 2-(5-nitro-1H-benzimidazol-2-yl)-3-(4-methoxyphenyl) acrylonitrile for copper corrosion in 1M nitric acid solution. This evaluation was conducted using gravimetric tests and density functional theory. The results proved that the inhibition power of this compound increases with the increase of reaction medium temperature, concentration and time of immersion. Adejo-Ekwenchi isotherm showed the existence of two modes adsorption: chemisorption and physisorption. In addition, this adsorption on copper surface conformed to modified Langmuir isotherm or Villamil model. It was proved that copper dissolution process is endothermic with disorders decrease. While activation thermodynamic parameters have attested that the adsorption on copper/solution interface is very favorable and stable with chemical adsorption predominance. Theoretical calculations showed that the good performance of the compound is due to its strong interaction with metal and which favors the covalent bonds formation. Thus, local parameters permitted to identify the reactivities sites of molecule.

Keywords: Copper, 2-(5-nitro-1H-benzimidazol-2-yl)-3-(4-methoxyphenyl) acrylonitrile, nitric acid, gravimetric tests, density functional theory

Introduction
Corrosion phenomenon is known and remains a major problem since the metals discovery, indeed this phenomenon contributes largely to their physical and chemical properties destruction of by making them unusable [1, 2]. Since then, research into means of protection has been observed in several structures using metals. This research has led to the development of protection several methods which are: protection by coatings, protection by electrochemical means and protection by inhibitors. These methods are applicable to the corrosion type [3]. In addition, the suitable solution must be compatible with the regulations concerning the protection of natural environment and must allow the recycling or disposal of individual components at the end of their use.

In order to reduce the rapid spread of metal corrosion in pickling shops, in mechanical and electronic industry, in petroleum industry (in oils and fuels), in pipelines and in food industry, corrosion inhibitors have been in great demand in recent years [4-8]. In fact, these inhibitors must permit to lower the metal corrosion rate, without affecting physico-chemical characteristics, they must be stable in presence of other constituents of environment, especially with respect to oxidants; they must be stable at the use temperatures of and be effective at low concentration and finally they must be compatible with the standards of non-toxicity and be inexpensive [9].

Thus, based on this information, the search for natural and synthesized inhibitors is necessary to reduce metals degradation. Among all metals, copper and its alloys have found an unlimited number of industrial applications such as in construction, engineering, automotive, plumbing, electrical, and electronic and other industrial applications, as they have remarkable functional properties [10].

Recently, many organic compounds have been used as copper corrosion inhibitors [11-14]. Their mechanism of action has been explained by the presence of heteroatoms and free electron pairs capable of facilitating their adsorption on copper surface. These explanations have often been reinforced by the density functional theory (DFT).

This theory has allowed to understand the specific sites of interaction between inhibitor and metal surface and to provide information of an organic inhibitor adsorption capacity on a metal surface that cannot be evaluated experimentally [15-17]. Adsorption of an organic inhibitor can affect the corrosion rate either by decreasing the available reaction zone (geometric blocking effect) or by changing the reaction activation energy.

Current study was designed to evaluate the inhibitory effect and adsorption properties of 2-(5-nitro-1H-benzimidazol-2-yl)-3-(4-methoxyphenyl) acrylonitrile of copper corrosion in 1M nitric acid solution. In addition, this work consists of checking temperature and time influence of studied molecule inhibition efficiency. The use of this series that is similar to benzimidazole derivatives, namely benzimidazolyl-2-arylacrylonitrile, is due to its therapeutic properties that it has displayed in the treatment of opportunistic mycotic infections that develop in humans or animals due to high chemoresistance that triazole derivatives presented [18, 19]. These therapeutic properties relate that it could be less toxic or not toxic.

Materials and Methods

Materials, solutions and inhibitor synthesis process

Experimental tests were carried out using copper material. Copper samples in the form of a rod measuring 10 mm long and 2 mm in diameter. They were cut from a pure copper (99.9%). The samples were then polished and abraded with abrasive papers (400, 600 and 800) washed thoroughly with distilled water, then degreased with acetone and rinsed with distilled water, before being dried in an oven at 80 °C. Copper sample, previously cleaned and dried, were weighed with an analytical balance (mass m_1) and finally stored in a moisture-free desiccator.

Analytical grade 65% nitric acid solution from Merck was used to prepare the corrosive aqueous solution of 1M concentration that served as the blank solution for all tests. Acetone from Sigma Aldrich with 99.5% purity was also used to degrease copper sample tests.

The compound 2-(5-nitro-1H-benzimidazol-2-yl)-3-(4-methoxyphenyl) acrylonitrile has molecular weight: 320.31 g/mol and its formula is $C_{17}H_{12}O_3N_4$.Using blank solution 1M HNO_3, four concentrations of this molecule were prepared. These concentrations are: 10^{-3} mM, 6.10^{-3} mM, 10^{-2} mM and 3.10^{-2} mM.

The synthesis method used for this molecule consists in reacting orthophenylenediamines with ethyl cyanoacetate used as reagent and solvent. The product obtained reacts with 4-methoxybenzaldehyde. The reaction is refluxed in anhydrous ethanol and in the presence of piperidine. The precipitate obtained is filtered and recrystallized in water. This synthesis is summarized by the following reaction mechanism.

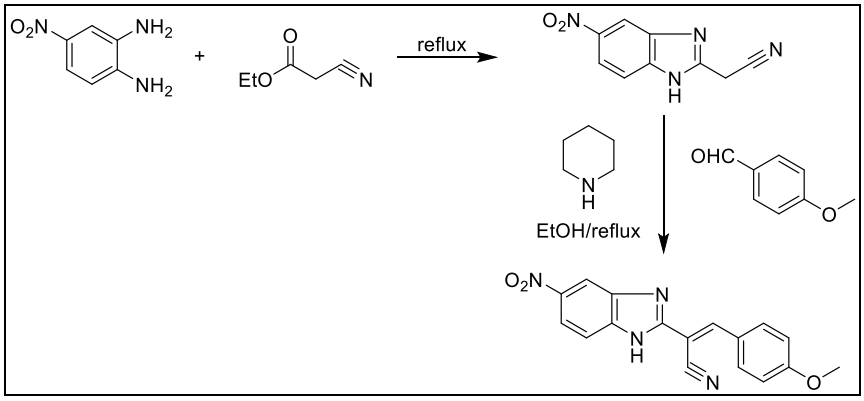

Physico-chemical properties Magnetic Resonance Nuclear (NMR) and mass spectroscopy are:

^{1}H NMR: (300 MHz, DMSO-*d6*, δ ppm): 13.67 (H, br s, NH); 8.39 (1H, s, C=CH); 3,92 (3H, s, CH3).

^{13}C NMR: (75 MHz, DMSO-*d6*, δ ppm): 142.97 (C=CH); 118.51 (C≡N); 97.79 (C=CH).

Gravimetric procedure

The samples were weighed and immersed completely in 50 mL in 1.0 M HNO_3 solution without or with the desired concentration of 2-(5-nitro-1H-benzimidazol-2-yl)-3-(4-methoxyphenyl) acrylonitrile. After one hour exposure in a thermostat water bath, the samples were removed from the solution, cleaned appropriately, dried, and reweighed using an analytical balance (precision: ± 0.1 mg), either m_2 the mass. The difference between the mass of the samples after exposure in corrosive solution and their initial mass was used to assess the mass loss. In order to study temperature effect on copper inhibition corrosion, the experimental tests were carried out at temperatures between 298 and 323K. To investigate influence time, immersion duration of one hour was extended to 2h, 3h and 4h. All tests were performed in triplicate in each case and the average value of mass loss was reported.

The corrosion rate was calculated from mass loss, it is expressed by:

$$W = \frac{\Delta m}{S.t} = \frac{m_1 - m_2}{S.t} \quad (1)$$

Δm: is mass loss (g), m_1 and m_2 are respectively mass (g) before and after immersion in solution test; t: immersion time (h); S: sample total surface (cm^2).

Studied molecule inhibition efficiency (IE) was evaluated from the following relation:

$$IE(\%) = \frac{W_0 - W}{W_0} * 100 \quad (2)$$

w_0 and w; are respectively copper corrosion rates in absence and presence of molecule.

Computational details for quantum chemical calculation

In the present work, quantum chemical calculations were performed using Gaussian 09 software [20]. These calculations were performed to establish correlations between molecular

structure and studied molecule inhibition efficiency. Density functional theory (DFT) method with B3LYP functional Becke's three parameter exchange functional, Lee–Yang–Parr) [21, 22], which is reliable enough for geometric optimizations combined with the split-valence double and triple zeta basis set 6-31G(d,p) and 6-311G(d,p) with two with two polarization functions (d and p orbitals). These polarization functions reveal that a d-type orbital has been added to all atoms except hydrogen atoms, and p-type orbital has been added to all hydrogen atoms. These basis sets were used to model the electronic properties of the studied compound and they are widely known because they provide accurate geometries and electronic properties for a large number of organic compounds. Optimized geometric of 2-(5-nitro-1H-benzimidazol-2-yl)-3-(4-methoxyphenyl) acrylonitrile with minimal energy realized through DFT at B3LYP/6-31G (d,p) is illustrated by Figure 1.

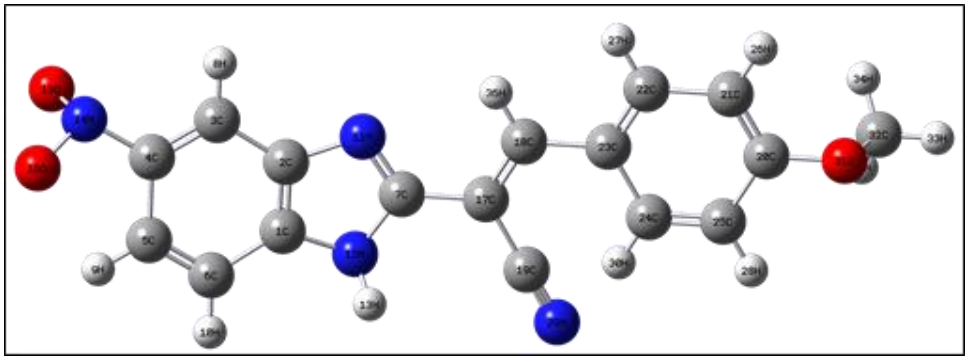

Fig 1: Optimised structure of 2-(5-nitro-1H-benzimidazol-2-yl)-3-(4-methoxyphenyl) acrylonitrile (NBMA)

These calculations provided access to the following global quantum chemical parameters: highest occupied molecular orbital energy (E_{HOMO}), lowest unoccupied molecular orbital energy (E_{LUMO}), energy gap (ΔE), dipole moment (μ), electron affinity (A), ionization energy (I), electronegativity (χ), hardness (η), softness (σ), electrophylicity index (ω), fraction of electron transferred (ΔN) and total energy (E_T). The reactivity sites analysis within the molecule was performed by the local quantities such as Fukui functions and dual descriptor. All these global and local reactivity parameters listed were computed. The expressions used to calculate these parameters are related as follows [23-25]:

$$\Delta E = E_{LUMO} - E_{HOMO} \quad (3)$$

$$I = -E_{HOMO} \quad (4)$$

$$A = -E_{LUMO} \quad (5)$$

$$\chi = -\mu_p = \left(\frac{\partial E}{\partial N}\right)_{v(r)} \quad (6)$$

$$\chi = \frac{I+A}{2} \quad (7)$$

$$\eta = \frac{I-A}{2} \quad (8)$$

$$\sigma = \frac{1}{\eta} = \frac{2}{I-A} \quad (9)$$

$$\omega = \frac{(I+A)^2}{4(I-A)} \quad (10)$$

$$\Delta N = \frac{\phi_{cu}-\chi_i}{2(\eta_{cu}+\eta_i)} \quad (11)$$

Where ϕ_{Cu}= 4.98 eV [26] and the hardness of copper η_{Cu}= 0 [27], χ_i and denote the electronegativity and η_i hardness of the inhibitor molecule.

$$f_k^+ = [q_k(N+1) - q_k(N)] \quad (12)$$

$$f_k^- = [q_k(N) - q_k(N-1)] \quad (13)$$

Where f_k^+ and f_k^- are respectively nucleophilic and electrophilic Fukui functions, $q_k(N+1)$, $q_k(N)$ and $q_k(N-1)$ are the electronic population of atom k in cationic, neutral and anionic forms [28].

Reactivity sites identification can be done without ambiguity with dual descriptor whose expression [29, 30] is:

$$\Delta f_k(r) = f_k^+ - f_k^- \quad (14)$$

Results and discussion

Gravimetric results analysis

Effect of temperature, inhibitor concentration and immersion time

The evolution of corrosion rate and inhibition efficiency of NBMA as a function of different concentrations and temperatures during gravimetric tests is given by Figures 2 and 3.

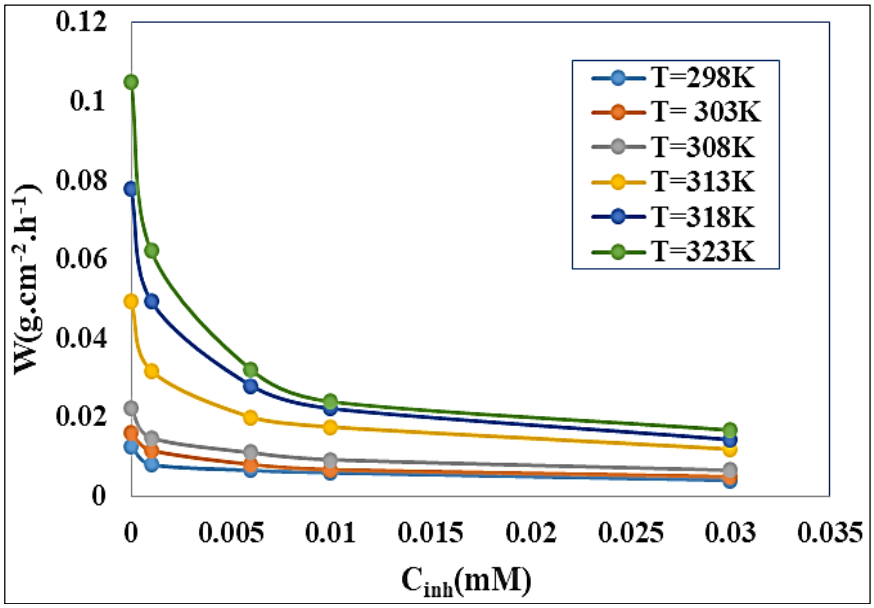

Fig 2: Corrosion rate versus concentrations for different temperatures

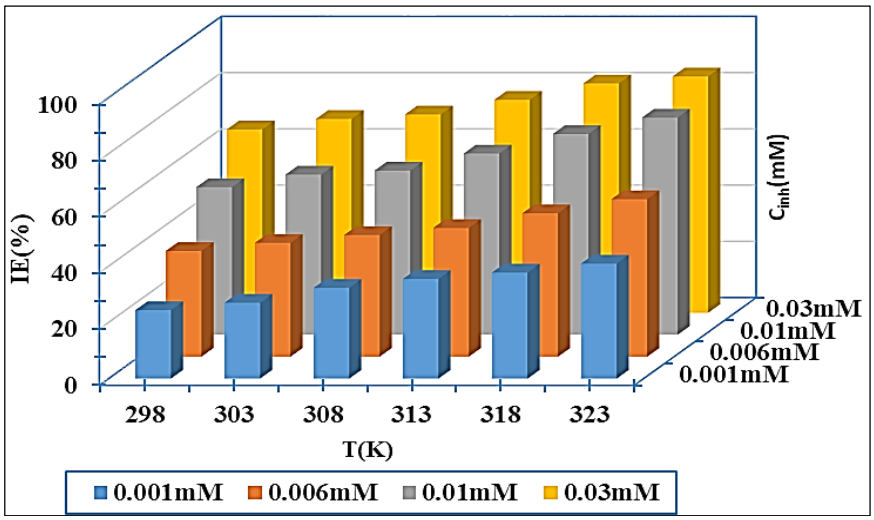

Fig 3: Inhibition efficiency (IE) versus temperature for different concentrations

Figure 4 shows inhibition efficiency evolution when immersion time evolves

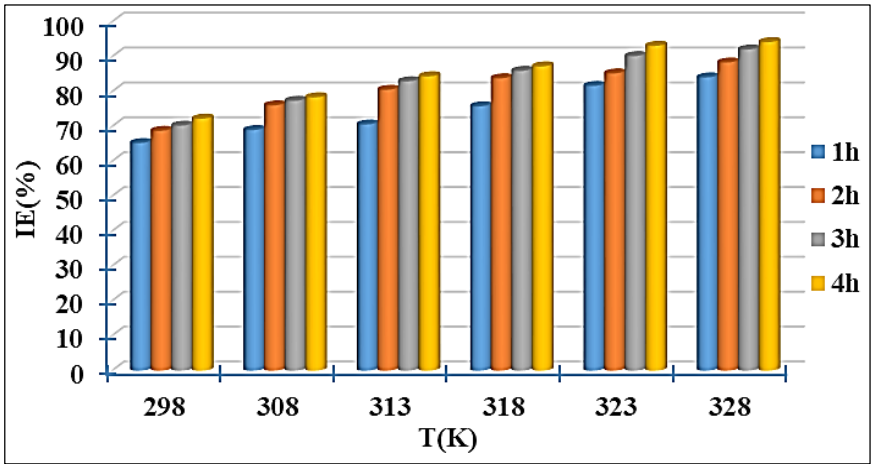

Fig 4: Inhibition efficiency (IE) versus immersion time for various concentration

Figures 2, 3 and 4 analysis relates that molecule studied inhibition efficiency was its concentration, corrosive medium temperature and immersion time dependent. Indeed, Figure 2 shows that for a given temperature copper corrosion rate decreases as the concentration of NBMA increases. It is also found that this rate increases with increasing reaction medium temperature. As in Figure 3, it is clear that the inhibition efficiency increases when the inhibitor concentration and

temperature increase. These observations attest that the molecule adsorbs on copper surface when temperature and inhibitor concentration evolve. This adsorption, which becomes more and more important when corrosive environment temperature increases, comes from inhibitor dissolution at high temperatures. A protective layer is then created on metal surface, which prevents corrosive solution from directly attacking copper, and this layer becomes thicker as inhibitor concentration increases. Similar observations have been obtained in previous works [31, 32]. Figure 4 clearly specifies that inhibition efficiency increases with immersion time, this reveals that the amount of molecules adsorbed on copper surface becomes more and more compact when immersion time increases. But the low deviation between the bands in the diagram after one hour immersion permits to deduce that one hour time is suitable for studying inhibition properties molecule. It can be seen that the studied molecule can significantly reduce the copper corrosion when the temperature and time rises.

Although surface coverage increases with temperature, NBMA concentration and immersion time, but this coverage does not cover the entire metal surface. These findings explain that despite NBMA presence in corrosive solution, the corrosion does not stop completely, so it simply reduced. Thus to explain this assertion, the corrosion process activation parameters were computed. The dependence of corrosion rate on temperature can be expressed by Arrhenius and transition state equations [33] which are illustrated by the next relationship:

$$logW = logA - \frac{E_a}{2.3.R.T} \quad (15)$$

$$log\left(\frac{W}{T}\right) = log\left(\frac{R}{\aleph.h}\right) + \frac{\Delta S_a^*}{2.3.R} - \frac{\Delta H_a^*}{2.3.R.T} \quad (16)$$

W: corrosion rate, E_a: activation energy of metal dissolution reaction, R: universal gas constant, T: temperature, A: Arrhenius preexponential constant.

ΔS_a^*: Activation entropy, ΔH_a^*: activation enthalpy, R universal gas constant, $\aleph$: Avogadro number, h: Planck's constant.

Activation energy was calculated from the slopes of $logW$ versus $\frac{1}{T}$ graph depicted (Figure 5). ΔH_a^* and ΔS_a^* were calculated from the slope and intercept, respectively, of the line plots from $log\left(\frac{W}{T}\right)$ versus $\frac{1}{T}$ (Figure 6). These activation parameters values are given by Table 1.

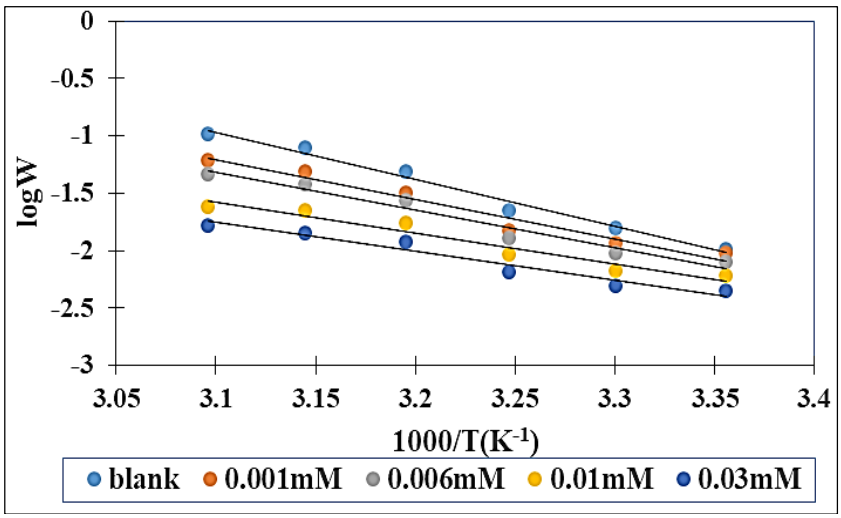

Fig 5: $logW$ versus $\frac{1}{T}$

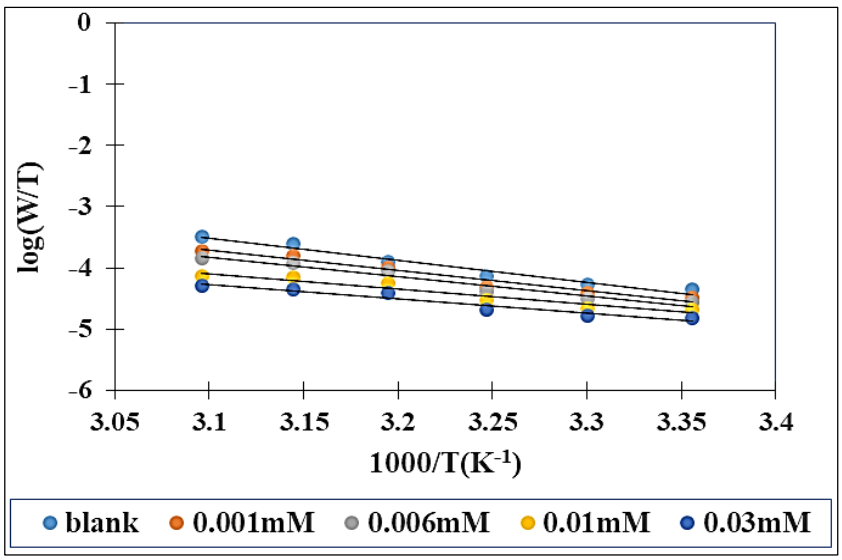

Fig 6: $log\left(\frac{W}{T}\right)$ versus $\frac{1}{T}$

Table 1: Copper dissolution parameters in 1M HNO_3

C_{inh} (mM)	$E_a(kJmol^{-1})$	$\Delta H_a^*(kJmol^{-1})$	$\Delta S_a^*(Jmol^{-1}K^{-1})$
0	72.03	69.42	-49.51
0.001	65.81	63.23	-72.61
0.006	62.53	59.95	-84.89
0.010	50.85	48.27	-126.13
0.030	47.75	45.18	-139.08

Table 1 examination indicates that activation energy (E_a) values in inhibited solutions are lower than in blank solution. This quantity expresses the energy amount to be supplied to corrosive solution to initiate copper dissolution. The decrease of this energy in inhibited solutions reveals that copper dissolution in these solutions is done with a lower energy than in blank solution. Under these conditions, it appears that NBMA presence in HNO_3 favors the establishment of a physical barrier on copper surface that reduces its dissolution. This barrier resulting from NBMA adsorption is favored by electronic exchanges between the metal and molecule which reflects chemical adsorption predominance [34].

ΔH_a^* positive values reflect the endothermic nature of copper dissolution process, indicating that this dissolution is very slow in NBMA presence [34]. In addition, the data collected in Tables 1 indicate that the average value of difference between E_a and ΔH_a^* is around 2.58 kJ mol^{-1} which equals the average value of RT (2.58 kJ.mol^{-1}).This result satisfies the thermodynamic equation which is: E_a- ΔH_a^* = RT. Previous studies have found similar results [35].

Activation entropy values are negative, suggesting the formation of a Cu-inh complex [34]. These values decrease when temperature increases revealing the decrease in disorder. This decrease comes from the amount of water substituted by inhibitor molecules which decreases when temperature increases.

Adsorption isotherm model research

The previous results state that molecule adsorbs on copper surface. Thus, molecular adsorption process at metal/solution interface by which inhibition phenomenon can be carried out is based on surface coverage rate (θ) whose expression is as follows:

$$\theta = \frac{W_0 - W}{W_0} \quad (3)$$

However, adsorption models series that are Langmuir, Temkin, El-Awady model were employed and examined to identify the isotherm that best fits coverage data of copper surface. The equations of the investigated isotherms are recorded in Table 2.

Table 2: Equations of the studied adsorption isotherms

Isotherm	Equation
Langmuir	$\frac{C_{inh}}{\theta} = \frac{1}{K_{ads}} + C_{inh}$
Temkin	$\theta = \frac{2.303}{f}[logK_{ads} + logC_{inh}]$
El-Awady	$log\left(\frac{\theta}{1-\theta}\right) = logK + ylogC_{inh}$

Where, C_{inh}: inhibitor concentration; K_{ads}: adsorption equilibrium constant; θ: surface coverage rate and $K_{ads} = K^{1/y}$

The plots corresponding to different isotherms studied are provided by Figures 7, 8 and 9.

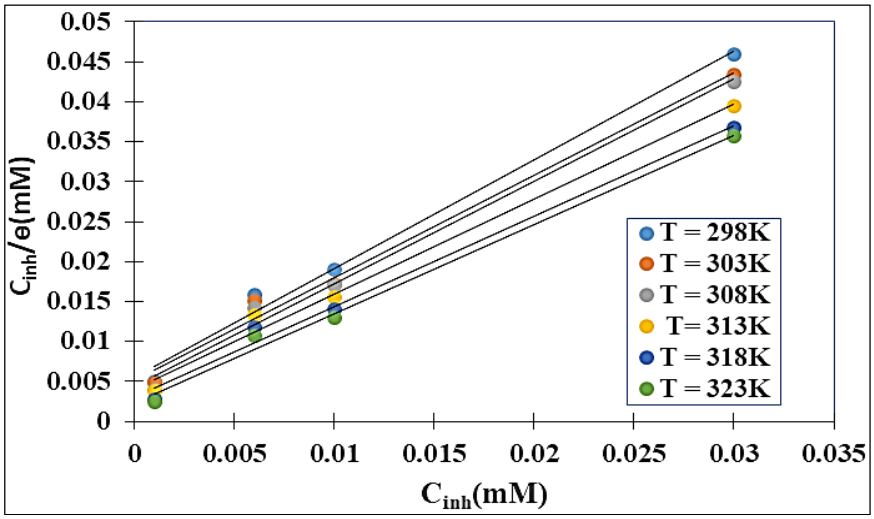

Fig 7: Langmuir adsorption isotherm plots for NBMA at different temperatures

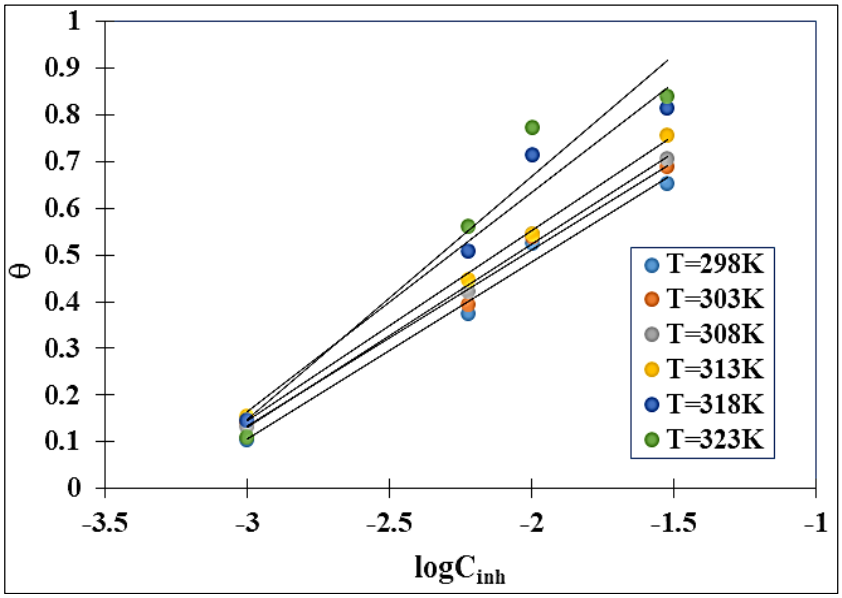

Fig 8: Temkin adsorption isotherm plots for NBMA at different temperatures

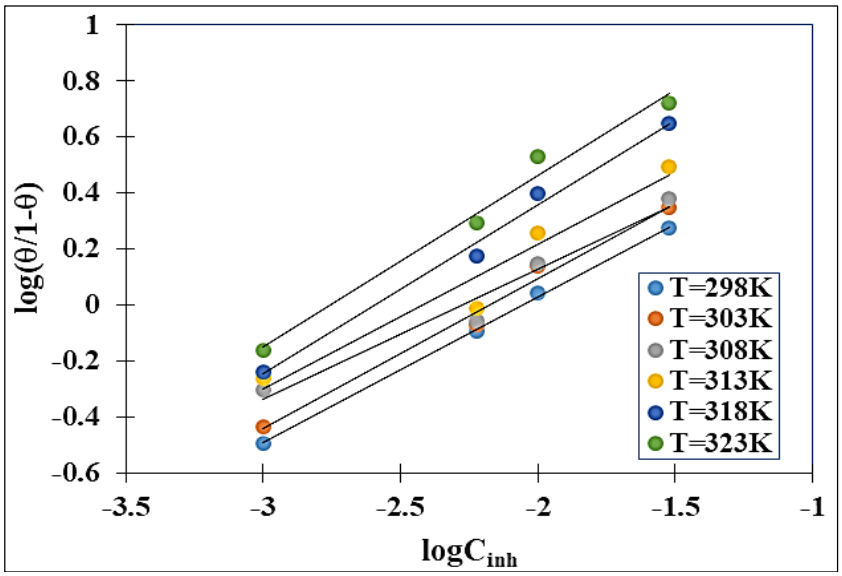

Fig 9: El-Awady adsorption isotherm plots for NBMA at different temperatures

Studied isotherms adsorption parameters are recorded in Table 3.

Table 3: Adsorptions isotherms parameters

Isotherm	T(K)	R^2	Intercept	Slope
Langmuir	298	0.9905	0.0055	1.3600
	303	0.9900	0.0051	1.2841
	308	0.9913	0.0044	1.2824
	313	0.9902	0.0041	1.1891
	318	0.9907	0.0030	1.1325
	328	0.9930	0.0023	1.1173
Temkin	298	0.9856	1.2438	0.3793
	303	0.9883	1.2676	0.3780
	308	0.9964	1.3085	0.3921
	313	0.9975	1.3646	0.4063
	318	0.9662	1.5772	0.4712
	328	0.9444	1.7095	0.5206
El-Awady	298	0.9991	1.072	0.5211
	303	0.9872	1.1693	0.5366
	308	0.9642	1.0552	0.4633
	313	0.9469	1.2528	0.5177
	318	0.9907	1.5713	0.6060
	328	0.9219	1.6884	0.6133

Table 4: Adsorption thermodynamic parameters

T(K)	K_{ads}(X10^{3}M^{-1})	$\Delta G^0_{ads}(kJ\ mol^{-1})$	$\Delta H^0_{ads}(kJ\ mol^{-1})$	$\Delta S^0_{ads}(J\ mol^{-1}K^{-1})$
298	181.8182	-39.936	27.71	226.2
303	196.0784	-40.797		
308	227.2727	-41.848		
313	243.9024	-42.711		
318	333.3333	-44.219		
323	434.7826	-45.627		

The choice of the suitable isotherm for this study is based on determination coefficients (R^2) of obtained straight lines. Determination coefficients of Langmuir isotherm are closer to unity (R^2 = 0.99), it results in this case that this isotherm is the best to describe NBMA behavior on copper surface. Although this isotherm is the best fit, it appears that the slopes of straight lines deviations are greater than unity. These deviations can be attributed to interactions between the adsorbed species. Finally, the analyses indicate that Langmuir isotherm cannot be applied in all its rigor, it is appropriate in this case that modified Langmuir isotherm or Villamil model [36] is more fitted and coherent to interpret NBMA adsorption on copper surface. This model is expressed as follows:

$$\frac{C_{inh}}{\theta} = \frac{n}{K_{ads}} + nC_{inh} \quad (17)$$

In this expression n takes considers the factors that were not taken into account by Langmuir isotherm, hence Langmuir isotherm parameters given in Table 3 are adapted to Villamil model.

Similar results have been obtained in literature [37]. However, multilayers are formed on copper surface with interactions between the adsorbed species, thus favoring a better protection, which is in agreement with the results obtained in this study.

Adsorption thermodynamic parameters Study

To study the molecule tested adsorption properties which related to copper corrosion, thermodynamic parameters were determined. These parameters are: standard adsorption free energy (ΔG^0_{ads}), standard adsorption enthalpy (ΔH^0_{ads}), standard adsorption entropy(ΔS^0_{ads}). ΔG^0_{ads} values were calculated from adsorption constant (K_{ads}) values. The values of this constant were determined from the parameters fitted to Villamil model in Table 3.So, the standard adsorption free energy (ΔG^0_{ads}) was computed, using the relation below [38]:

$$\Delta G^0_{ads} = -RTln(55.5\ K_{ads}) \quad (18)$$

Where R is gas constant, T is absolute temperature, K_{ads} adsorption equilibrium constant and 55.5 is water concentration (mol/L) in solution.

ΔH^0_{ads} and ΔS^0_{ads} were determined from the equation:

$$\Delta G^0_{ads} = \Delta H^0_{ads} - T\Delta S^0_{ads} \quad (19)$$

Plotting ΔG^0_{ads} versus temperature (Figure 10) allows to calculate these two adsorption parameters. The different values reported in Table 4.

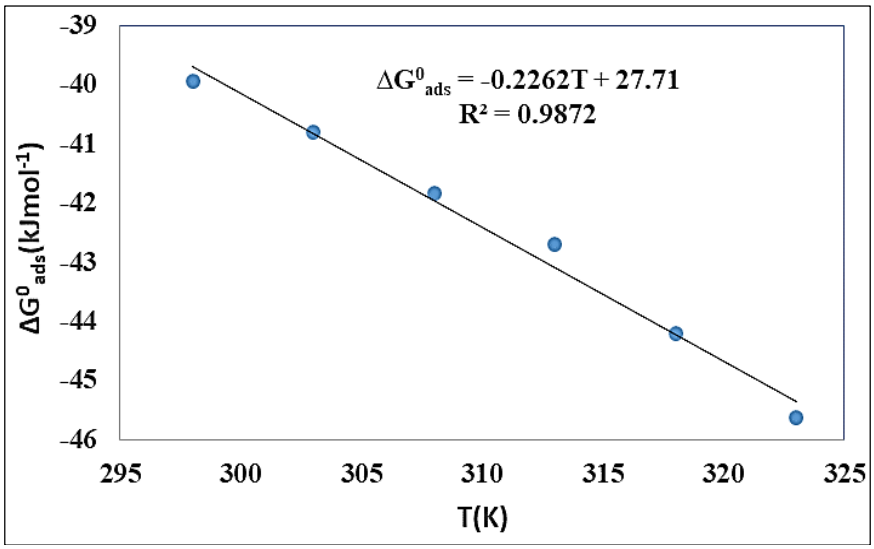

Fig 10: ΔG^0_{ads} versus temperature

Adsorption equilibrium constant values (K_{ads}) increase as the temperature increases, implying a strong NBMA adsorption capacity on copper surface as the temperature increases. ΔG^0_{ads} positive values unveil that the adsorption on copper/solution interface is favorable, and this leads to better inhibition [39]. This quantity allows to judge adsorption type. Indeed according to previous studies [40, 41], if $\Delta G^0_{ads} \geq -20kJ.mol^{-1}$, adsorption is physical (electrostatic interactions), if $\Delta G^0_{ads} \leq -40kJ.mol^{-1}$, we have a chemical adsorption (covalent bonds) and if $-40kJ.mol^{-1} \leq \Delta G^0_{ads} \leq -20kJ.mol^{-1}$ inhibitor adsorption involves both chemical and physical adsorption. In this study, one value of ΔG^0_{ads} obtained (-39.936 KJ.mol^{-1}) is less than -20 kJ.mol^{-1}, while the other values are less than -40 kJ.mol^{-1}. These results show that both chemical and physical adsorptions are formed in metal/solution interface during copper corrosion inhibition process [42]. These results clearly reveal that chemical adsorption is predominant. The adsorption process is endothermic because $\Delta H^0_{ads} > 0$. ΔS^0_{ads} Positive value detects that the messy increases during NBMA molecules adsorption,

this messy is justified by water molecules desorption on metal surface [43].

The standard adsorption free energy values analysis indicate that chemical and physical adsorption are involved during the adsorption process. In order to better attest adsorption nature, Adejo-Ekwenchi adsorption isotherm whose equation is written as follows was used [44].

$$log\left(\frac{1}{1-\theta}\right) = logK_{AE} + blogC_{inh} \quad (20)$$

Where θ and C_{inh} are respectively the fraction of surface coverage and the inhibitor concentration, K_{AE} and b are the isotherm parameters.

The corresponding plots of $log\left(\frac{1}{1-\theta}\right)$ versus $logC_{inh}$ and linear fitted straight lines are given in Figure 11. The parameters corresponding to this isotherm are reported in Table 5.

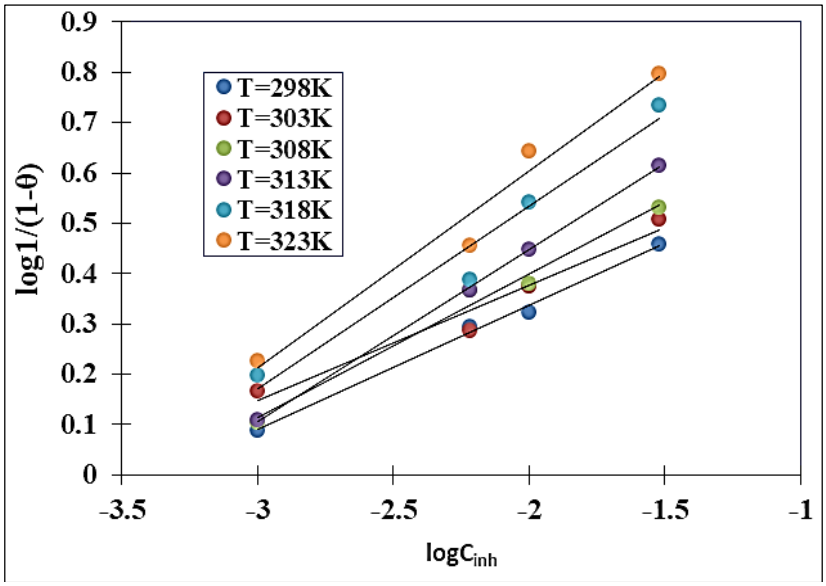

Fig 11: $log\left(\frac{1}{1-\theta}\right)$ versus $logC_{inh}$

Table 5: Adejo-Ekwenchi adsorption isotherm parameters

T(K)	Equation	R^2	b	K_{AE}
298	$log\left(\frac{1}{1-\theta}\right) = 0.2467logC_{inh} + 0.8313$	0.9947	0.2467	6.7810
303	$log\left(\frac{1}{1-\theta}\right) = 0.2227logC_{inh} + 0.8374$	0.9923	0.2227	6.8770
308	$log\left(\frac{1}{1-\theta}\right) = 0.2849logC_{inh} + 0.9694$	0.9843	0.2849	9.3196
313	$log\left(\frac{1}{1-\theta}\right) = 0.3424logC_{inh} + 1.1345$	0.9996	0.3424	13.6301
318	$log\left(\frac{1}{1-\theta}\right) = 0.3635logC_{inh} + 1.2618$	0.9633	0.3635	18.2725
323	$log\left(\frac{1}{1-\theta}\right) = 0{,}3928logC_{inh} + 1{,}3905$	0.9699	0.3928	24.5754

Parameter b value decreases in the temperature range from 298K to 303K.This decrease reveals that in this temperature interval NBMA adsorbs on copper surface by electrostatic bonds. On the other hand, from 303K to 323K, parameter b values increase, thus implying chemisorption [44]. It results in this case that molecule adsorbs on copper by covalent bonds from 303K to 323K. These bonds are strong at high temperatures, thus justifying inhibition efficiency high values obtained when the temperature increases. It appears that K_{AE} values increase when temperature rises, confirming NBMA strong adsorption on copper at high temperature.

Quantum chemical parameters analysis

Global reactivity parameters determined by means of DFT at B3LYP/6-31G (d,p) and B3LYP/6-311G(d,p) are listed in Table 6.

Table 6: Computation quantum chemical of NBMA parameters by B3LYP at 6-311G (d,p) and 6-311G (d,p)

Parameters	6-31G(d,p)	6-311G(d,p)
E_{HOMO} (eV)	-6.215	-6.595
E_{LUMO} (eV)	-2.699	-3.342
ΔE (eV)	3.515	3.252
μ (Debye)	3.813	3.934
I (eV)	6.214	6.595
A (eV)	2.699	3.342
χ(eV)	4.457	4.969
η(eV)	1.758	1.626
$\sigma(eV)^{-1}$	0.569	0.614
ΔN	0.149	0.003
ω	5.652	7.592
E_T (Ha)	-1099.6	-1099.8

Quantum chemical parameters of a molecule are descriptors that permit to judge and explain correctly the reactivity of an organic compound [45, 46]. Indeed, experimental results analysis showed that the good inhibiting performances of NBMA are due to its capacity to adsorb on copper surface. Although the inhibiting effect of NBMA in copper corrosion is proved by gravimetric tests, however these gravimetric tests could not explain well the mechanism of adsorption of this molecule on copper surface. In this part, it is necessary to explain how this adsorption is done. The electron density distribution of HOMO and LUMO orbitals of NBMA realized by means of DFT at B3LYP/6-31G (d,p) is described by Figure 12. This Figure clearly indicates that the electronic distribution is more on the heteroatoms (O and N), double and triple bonds, confirming that these sites are able to give electrons to the empty copper orbitals to establish covalent bond.

According to theory frontier orbitals, the molecule ability to give or receive electrons depends on its highest occupied molecular orbital energy (E_{HOMO}) and its lowest unoccupied molecular orbital energy (E_{LUMO}) [47, 48]. In fact, a high value of E_{HOMO} notifies that molecule gives electrons to a compound with a lower orbital energy. While a low value of E_{LUMO} certifies that molecule has strong electron acceptor properties. Referring to previous works [49, 50], NBMA has a high value of E_{HOMO} and a low value of E_{LUMO}, this reflects the strong ability that NBMA has to give and receive electrons from copper. Indeed, since copper electronic structure is $[Ar]3d^{10}4s^{1}$, 4s orbital is incompletely filled and unfilled 4p orbital can form coordination bonds with the electrons in NBMA HOMO orbital, while the electrons in completely filled 3d orbital can react with NBMA LUMO orbital. Copper ions Cu^{2+} emanating from copper corrosion and having an electronic structure ($[Ar]3d^{9}$) can receive electrons from NBMA HOMO orbital to form coordination bonds, which bonds will form a protective film on metal surface that will effectively inhibit copper corrosion.

Energy gap between LUMO and HOMO (ΔE) is an important parameter to assess an inhibitor reactivity and its adsorption on metal surface [51]. The reactivity of a molecule increases with decreasing ΔE thus leading to higher inhibition A

The literature reports that there are disagreements in dipole moment (μ) use to interpret the inhibition properties of an organic compound [52, 53]. Face many disagreements this parameter cannot be used to analyze NBMA behavior.

NBMA electronegativity value χ = 4.969eV is lower than that of copper (χ_{Cu}=4.98eV), which makes the value of electron transferred fraction positive the fraction (ΔN >0), so NBMA adsorption on copper surface is probably based on the high tendency of NBMA to donate electrons to copper [54]. NBMA electron-donating character slows down copper oxidation by considerably reducing its corrosion. Similar results were obtained by Issaadi *et al.* [55].

The inhibition effect of an organic compound depends on its reactivity character. This character can be judged by the values of η and σ. According to previous results available [24, 56] in the literature, NBMA has a high value of softness (σ) and a low of hardness (η), so it is suitable that NBMA is highly reactive which justifies its good anticorrosive properties. All these theoretical indicators correlate perfectly with experimental results.

To identify the nucleophilic and electrophilic character, Parr *et al.* [57] proposed the electrophilicity index (ω), according to their studies, NBMA has a low value of ω which endorses the electrophilic character revealed by the value of E_{LUMO}.

E_T value mentions that NBMA is stable in studied medium and this stability favors its ability to give electrons to copper which confirms experimental values obtained [53].

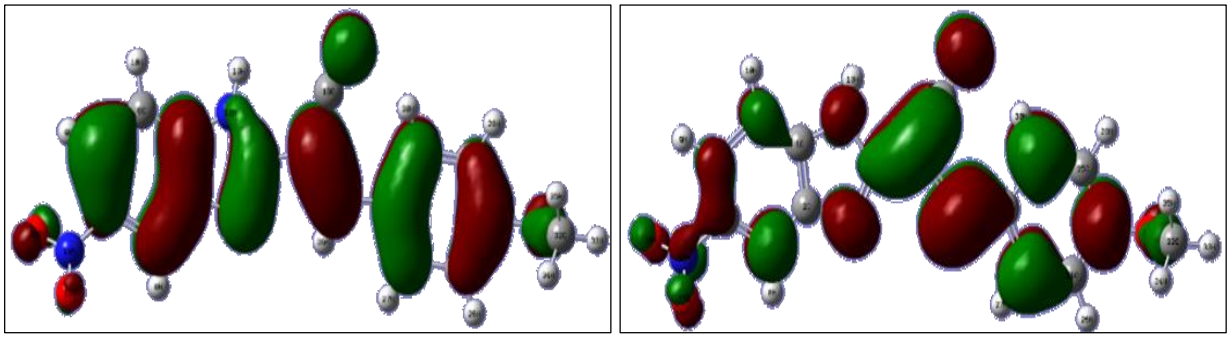

NBMA HOMO orbital **NBMA LUMO orbital**

Electronic transfer between NBMA and copper surface, CB: Conduction band, VB: Valence band

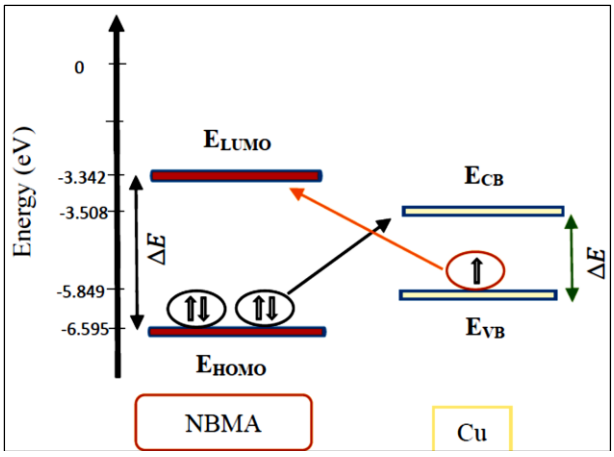

Fig 12: HOMO and LUMO orbital of NBMA, Electronic transfer between NBMA and copper surface schematic

Global parameters confirmed NPMA good inhibition performance which was detected by experimental results. This good reactivity emanates from its better electron donor and acceptor character. Therefore, it is necessary to elucidate the sites on which these electronic transactions take place, in this case it is important to prove the probable sites of nucleophilic and electrophilic attacks. The identification of these sites was possible thanks to the local reactivity descriptors that are Fukui functions (f_k^+, f_k^-) and dual descriptor $\Delta f_k(r)$. The values of these local parameters are recorded in Table 7.

Table 7: Mulliken atomic charges and Local reactivity parameters of NBMA

Atoms	$q_k(N+1)$	$q_k(N)$	$q_k(N-1)$	f_k^+	f_k^-	$\Delta f_k(\mathbf{r})$
1C	0.14968	0.216304	-0.015479	-0.066624	0.231783	-0.298407
2C	0.064475	0.207811	-0.000541	-0.143336	0.208352	-0.351688
3C	-0.044015	-0.093577	0.007315	0.049562	-0.100892	0.150454
4C	0.054234	0.238323	0.024808	-0.184089	0.213515	-0.397604
5C	0.117116	-0.060932	0.005946	0.178048	-0.066878	0.244926
6C	-0.05664	-0.104348	0.003022	0.047708	-0.10737	0.155078
7C	0.01968	0.442329	0.011229	-0.422649	0.4311	-0.853749
8H	0.001512	0.134064	0.001497	-0.132552	0.132567	-0.265119
9H	-0.004927	0.135143	0.002773	-0.14007	0.13237	-0.27244
10H	0.001666	0.120363	0.001378	-0.118697	0.118985	-0.237682
11N	0.081168	-0.539201	0.018682	0.620369	-0.557883	1.178252
12N	0.000643	-0.588778	-0.001186	0.589421	-0.587592	1.177013
13H	-0.000608	0.282502	-0.000154	-0.28311	0.282656	-0.565766
14N	-0.012348	0.128012	0.238607	-0.14036	-0.110595	-0.029765
15O	0.056896	-0.268157	0.346479	0.325053	-0.614636	0.939689
16O	0.010395	-0.279487	0.169171	0.289882	-0.448658	0.73854
17C	0.157784	0.045904	0.0123	0.11188	0.033604	0.078276
18C	-0.004258	-0.088191	0.113643	0.083933	-0.201834	0.285767
19C	-0.026191	0.323304	0.000359	-0.349495	0.322945	-0.67244
20C	0.165391	0.310127	0.035255	-0.144736	0.274872	-0.419608
21C	0.025476	-0.113488	-0.01859	0.138964	-0.094898	0.233862
22C	0.057191	-0.154307	0.047776	0.211498	-0.202083	0.413581
23C	0.128993	0.09473	-0.019083	0.034263	0.113813	-0.07955
24C	0.0235	-0.085609	0.018039	0.109109	-0.103648	0.212757
25C	-0.021169	-0.13879	-0.014336	0.117621	-0.124454	0.242075
26H	-0.001657	0.103056	0.000646	-0.104713	0.10241	-0.207123
27H	-0.002955	0.102149	-0.00219	-0.105104	0.104339	-0.209443
28H	0.000267	0.105709	0.000517	-0.105442	0.105192	-0.210634
29N	0.032193	-0.498552	0.017646	0.530745	-0.516198	1.046943
30H	-0.001652	0.137007	-0.001038	-0.138659	0.138045	-0.276704
31O	0.021327	-0.530181	-0.000614	0.551508	-0.529567	1.081075
32C	0.00611	-0.071527	0.000952	0.077637	-0.072479	0.150116
33H	0.000777	0.12265	0.000395	-0.121873	0.122255	-0.244128
34H	0.00011	0.106316	-0.00001	-0.106206	0.106326	-0.212532
35H	0.000458	0.109346	0.000006	-0.108888	0.10934	-0.218228
36H	-0.000622	0.149976	-0.005221	-0.150598	0.155197	-0.305795

Table 7 exploration reveals that atom C(7) has the highest value of f_k^- and the lowest value of $\Delta f_k(r)$, while atom N(11) has the highest value of f_k^- and $\Delta f_k(r)$. According to Parr *et al*. [58] and Martínez-Araya and associates [30], C(7) and N(11) are likely sites for electrophilic and nucleophilic attacks, respectively. These sites which are associated respectively with HOMO and LUMO orbitals of the studied molecule identify donation and reception electron centers.

Conclusion

Theoretical and experimental combination have certified that 2-(5-nitro-1H-benzimidazol-2-yl)-3-(4 methoxyphenyl) acrylonitrile can be used to inhibit copper corrosion in 1M nitric acid solution. Indeed, its inhibition efficiency depends on its concentration, the reaction medium temperature and the immersion time, which inhibition efficiency reaches 84.09% at T = 323K with C_{inh} = 0.03mM. Different isotherms inspection showed that the adsorbed quantity obeys to Villamil adsorption model and involves both physisorption and chemisorption. Activation parameters analysis showed that chemisorption is predominant, marked by Cu-inh complex formation during which the disorder decreases. As for the thermodynamic adsorption parameters, they evoke that the adsorption process is spontaneous, endothermic, and accompanied by an increase in disorder. It was shown by quantum chemical parameters (E_{HOMO}, E_{LUMO}, ΔE, ΔN, χ, σ, η) that this good performance is due to NBMA strong adsorption on copper surface. This adsorption comes from the coordination bonds formation with copper, where the main adsorption centers that are susceptible to nucleophilic and electrophilic attacks were identified using Fukui and dual descriptor functions. These are C(7) and N(11) atoms, respectively. The results obtained by quantum chemical calculations coincide well with experimental data, which confirms that these theoretical calculations permitted to judge and explain correctly NBMA reactivity in studied solution.

Acknowledgements

We express our gratitude of Environmental Sciences and Technologies Laboratory at Jean Lorougnon guede University of Daloa (Côte d'Ivoire) and the Laboratory of Constitution

and Reaction of Matter of Felix Houphouët Boigny university of Abidjan (Côte d'Ivoire).

References

1. Xu Y, Liu L, Zhou Q, Wang X, Huang Y. Understanding the influences of precorrosion on the erosion-corrosion performance of pipeline steel. Wear. 2020;442:203-151.
2. Popoola LT, Grema AS, Latinwo GK, Gutti B, Balogun AS. Corrosion problems during oil and gas production and its mitigation. International Journal of Industrial Chemistry. 2013;4(35):1-15.
3. Li XG, Zhang DW, Liu ZY, Li Z, Du CW, Dong CF. Share corrosion data. Nature. 2015;527:441-442.
4. Yul Ryu H, Ho Lee C, Uck Lee S, Nagendra SH, Yerriboina P, Jin Goo P. Theoretical validation of inhibition mechanisms of benzotriazole with copper and cobalt for CMP and post-CMP cleaning applications. Microelectronic Engineering. 2022;262:111-833.
5. Qiang Y, Zhang S, Guo L, Xu S, Feng L, Obot IB, *et al*. Sodium dodecyl benzene sulfonate as a sustainable inhibitor for zinc corrosion in 26% NH4Cl solution. Journal of Cleaner Production. 2017;152:17-25.
6. Rajkumar G, Gopalakrishnan SM. Corrosion protection ability of self-assembled monolayer of 3-amino-5-mercapto-1, 2, 4-triazole on copper electrode. Thin Solid Films. 2014;562:32-36.
7. Padash R, Sadat Sajadi G, Hamid Jafari A, Jamalizadeh E, Shokuhi Rad A. Corrosion control of aluminum in the solutions of NaCl, HCl and NaOH using 2,6-dimethylpyridine inhibitor: Experimental and DFT insights. Materials Chemistry and Physics. 2020;244:122-681.
8. Haoran L, Baoguo Z, Ye L, Pengfei W, Ye W, Mengchen X. Effect of novel green inhibitor on corrosion and chemical mechanical polishing properties of cobalt in alkaline slurry. Materials Science in Semiconductor Processing. 2022;146:106-691.
9. Mahdi BS, Aljibori HSS, Abbass MK, Al-Azzawi WK, Kadhum AH, Hanoon MM, *et al*. Gravimetric analysis and quantum chemical assessment of 4-aminoantipyrine derivatives as corrosion inhibitors. International Journal of Corrosion and Scale Inhibition. 2022;11(3):1191-1213.
10. Zhang X, He W, Odnevall WI, Leygraf C. Mechanistic studies of corrosion product flaking on copper and copper-based alloys in marine environments. Corrosion Science. 2014;85:15-25.
11. Tigori MA, Koné A, Mireille KA, Sissouma D, Niamien PM. Experimental and Theoretical Assessments on Anticorrosion Performance of 2-(1H-benzimidazol-2-yl)-3-(4-hydroxyphenyl) Acrylonitrile for Copper in 1M HNO_3. Earthline Journal of Chemical Sciences. 2022;9(1):17-45.
12. Yujie Q, Shengtao Z, Song Y, Xuefeng Z, Shijin C. Three indazole derivatives as corrosion inhibitors of copper in a neutral chloride solution. Corrosion Science. 2017;126:295-304.
13. Galai M, Rbaa M, Ouakki M, Dahmani K, Kaya S, Arrousse N, *et al*. Functionalization effect on the corrosion inhibition of novel ecofriendly compounds based on 8-hydroxyquinoline derivatives: Experimental, theoretical and surface treatment, Chemical Physics Letters. 2021;776:138-700.
14. Guo L, Tan B, Zuo X, Li W, Leng S, Zheng X. Eco-friendly food spice 2- Furfurylthio-3-methylpyazine as an excellent inhibitor for copper corrosion in sulfuric acid medium. Journal of Molecular Liquids. 2020;317:113-915.
15. Xu Y, Zhang S, Li W, Guo L, Xu S, Feng Li, *et al*. Experimental and theoretical investigations of some pyrazolo-pyrimidine derivatives as corrosion inhibitors on copper in sulfuric acid solution. Applied Surface Science. 2018;459:612-620.
16. Benhiba F, Hsissou R, Benzekri Z, Echihi S, El-Blilak J, Boukhris C, *et al*. DFT/electronic scale, MD simulation and evaluation of 6-methyl-2-(p-tolyl)-1,4-dihydroquinoxaline as a potential corrosion inhibition. Journal of Molecular Liquids. 2021;335:116-539.
17. Tigori MA, Kouyaté A, Kouakou V, Niamien PM, Trokourey A. Inhibition Performance of Some Sulfonylurea on Copper Corrosion in Nitric Acid Solution Evaluated Theoretically by DFT Calculations. Open Journal of Physical. Chemistry. 2020;10(3):139-157.
18. Smagill S, Shields C, Sears CL, Choti M, Merz W G. Résistance croisée aux dérivés triazolés chez Candida.: Observation, fréquence dans les isolats sanguins et implications pour les traitements antifongiques. Journal de mycologie médicale. 2007;17:S1-S10.
19. Djohan V, Angora KE, Vanga Bosson AH, Konaté A, Kassi FK, Yavo W, *et al*. *In vitro* susceptibility of vaginal *Candida albicans* to antifungal drugs in Abidjan (Ivory Coast). Journal de Mycologie Médicale. 2012;22(2):129-133.
20. Frisch MJ, Trucks GW, Schlegel HB, Scuseria GE, Robb MA, Cheeseman JR, *et al*. Fox. Gaussian (Gaussian, Inc., Wallingford CT); c2009, 09.
21. Becke D. Density functional calculations of molecular bond energies. The Journal of Chemical Physics. 1984;84:4524-4529.
22. Lee C, Yang W, Parr RG. Development of the Colle-Salvetti correlation-energy formula into a functional of the electron density. Physical Review B. 1988;37:785-789.
23. Koopmans T, Über Diet. Zuordnung von Wellenfunktionen und Eigenwerten zu den Einzelnen Elektronen Eines. Atoms Physica. 1934;1(1-6):104-113.
24. Abdallah M, Al-Bahir A, Altass HM, Fawzy A, El-Guesmi N, Arej S Al-Gorair, *et al*. Anticorrosion and adsorption performance of expired antibacterial drugs on Sabic iron corrosion in HCl solution: Chemical, electrochemical and theoretical approach. Journal of Molecular Liquids. 2021;330:115-702.
25. Behnaz H, Khanlarkhani A, Seyed MM, Arash Fattah-alhosseini A, Seyed OG. Evaluation of Henna Extract Performance on Corrosion Inhibition of API 5L Steel in H2S-Containing Medium and DFT Quantum Computing of Its Constituents. Metals and Materials International. 2020;27:4463-4476.
26. Michelson H. The work function of the elements and its periodicity. Journal of Applied Physics. 1977;48:4729-4733.
27. Dewar MJS, Zoebisch EG, Healy EF, Stewart JP. Development and use of quantum mechanical molecular models. 76. AM1: a new general purpose quantum mechanical molecular model. Journal of the American Chemical and Society. 1985;107:3902.
28. Guerrab W, Chung IM, Kansiz S, Mague JT, Dege N, Taoufik J, *et al*. Synthesis, structural and molecular characterization of 2,2-diphenyl-2H,3H,5H,6H,7H-

imidazo[2,1-b][1,3]thiazin-3-one. Journal of Molecular Structure. 2019;1197:369-376.
29. Morell C, Grand A, Toro-Labbé A. New Dual Descriptor for Chemical Reactivity. Journal of Physical Chemistry A. 2005;109:205-212.
30. Martinez-Araya JI. Why Is the Dual Descriptor a More Accurate Local Reactivity Descriptor than Fukui Functions? Journal of Mathematical Chemistry. 2015;5:451-465.
31. Jmiai A, Tara A, El-Issami S, Hilali M, Jbara O, Bazzi L. A new trend in corrosion protection of copper in acidic medium by using Jujube shell extract as an effective green and environmentally safe corrosion inhibitor: Experimental, quantum chemistry approach and Monte Carlo simulation study, Journal of Molecular Liquids. 2021;322:114-509, 1-36.
32. Echihi S, Benzbiri N, Belghiti ME, El-Fal M, Boudali M, Essassi EM *et al*. Corrosion inhibition of copper by pyrazole pyrimidine derivative in synthetic seawater: Experimental and theoretical studies. Materials today Proceedings. 2021;2:3958-3966.
33. Bashir S, Thakur A, Lgaz H, Chung IM, Ashish K. Corrosion Inhibition Performance of Acarbose on Mild Steel Corrosion in Acidic Medium: An Experimental and Computational Study. Arabian Journal for Science and Engineering. 2020;45:4773-4783.
34. Shaban SM, Abd-Elaal AA, Tawfik SM. Gravimetric and electrochemical evaluation of three nonionic dithiol surfactants as corrosion inhibitors for mild steel in 1 M HCl solution. Journal of Molecular Liquids. 2016;216:392-400.
35. Rahmani H, Alaoui KI, EL-Azzouzi M, Benhiba F, El-Hallaoui A, Rais Z, *et al*. Corrosion assessment of mild steel in acid environment using novel triazole derivative as an anti-corrosion agent: A combined experimental and quantum chemical study. Chemical Data Collections. 2019;24:100-302.
36. Villamil RFV, Corio P, Rubin JC, Agostinho SML. Effect of sodium dodecyl sulfate on copper corrosion in sulfuric acid media in the absence and presence of benzotriazole. Journal of Electro Analytical Chemistry. 1999;472:112-116.
37. Obot IB, Umoren SA, Gasem ZM, Suleiman R, El Ali B. Theoretical prediction and electrochemical evaluation of 2 vinylimidazole and allylimidazole as corrosion inhibitors for mild steel 3 in 1 M HCl. Journal of Industrial and Engineering Chemistry. 2015;21:1328-1339.
38. Qiang Y, Zhang S, Guo L, Zheng X, Xiang B, Chen S. Experimental and theoretical studies of four allyl imidazolium-based ionic liquids as green inhibitors for copper corrosion in sulfuric acid. Corrosion Science. 2017;119:68-78.
39. Zhoua L, Zhanga S, Tana B, Fenga L, Xianga B, Chena F, *et al*. Phenothiazine drugs as novel and eco-friendly corrosion inhibitors for copper in sulfuric acid solution. Journal of the Taiwan Institute of Chemical Engineers. 2020;113:253-263.
40. Haijun H, Yan F, Fuhua L, Zhenqiang W, Shengtao Z, Xinchao W, *et al*. Orderly self-assembly of new ionic copolymers for efficiently protecting copper in aggressive sulfuric acid solution. Chemical Engineering Journal. 2020;384:123-293.
41. Wang C, Lai C, Xie B, Guo X, Fu D, Li B, *et al*. Corrosion inhibition of mild steel in HCl medium by S-benzyl-O,O'-bis(2-naphthyl)dithiophosphate with ultra-long lifespan. Results in Physics. 2018;10:558-567.
42. Tan B, Zhang S, Qiang Y, Li W, Hao L, Feng L, *et al*. Experimental and theoretical studies on the inhibition properties of three diphenyl disulfide derivatives on copper corrosion in acid medium. Journal of Molecular Liquids. 2020;298:111-975.
43. Zhang GA, Hou XM, Hou BS, Liu HF. Benzimidazole derivatives as novel inhibitors for the corrosion of mild steel in acidic solution: Experimental and theoretical studies. Journal of Molecular Liquids. 2019;278:413-427.
44. Adejo SO, Ekwenchi MM. Resolution of adsorption characterisation ambiguity through the Adejo-Ekwenchi adsorption isotherm: a case study of leaf extract of Hyptis suaveolens poit as green corrosion inhibitor of corrosion of mild steel in 2 M HCl. Journal of Emerging Trends in Engineering and Applied Sciences. 2014;5:201-205.
45. Gao L, Peng S, Huang X, Gong Z. A combined experimental and theoretical study of papain as a biological eco-friendly inhibitor for copper corrosion in H_2SO_4 medium. Applied Surface Science. 2020;511:145-446.
46. Chen S, Zhao H, Chen S, Wen P, Wang H, Li W. Camphor leaves extract as a neoteric and environment friendly inhibitor for Q235 steel in HCl medium: combining experimental and theoretical researches. Journal of Molecular Liquids. 2020;312:113-433.
47. Albayati M, Kansız S, Dege N, Kaya S, Marzouki R, Lgaz H, *et al*. Synthesis, crystal structure, Hirshfeld surface analysis and DFT calculations of 2-[(2,3-dimethylphenyl)amino]-N'-[(E)-thiophen-2-ylmethylidene]benzohydrazide. Journal of Molecular Structure. 2020;1205:127-654.
48. Tabatabaei Majd M, Akbarzadeh S, Ramezanzadeh M, Bahlakeh G, Ramezanzadeh B. A detailed investigation of the chloride-induced corrosion of mild steel in the presence of combined green organic molecules of Primrose flower and zinc cations. Journal of Molecular Liquids. 2020;297:111-862.
49. Tan B, Zhang S, Qiang Y, Li W, Liu H, Xu C, *et al*. Insight into the corrosion inhibition of copper in sulfuric acid via two environmentally friendly food spices: combining experimental and theoretical methods. Journal of Molecular Liquids. 2019;286:110-891.
50. Qiang Y, Zhang S, Xu S, Li W. Experimental and theoretical studies on the corrosion inhibition of copper by two indazole derivatives in 3.0% NaCl solution, Journal of Colloid and Interface Science. 2016;472:52-59.
51. Bahlakeh G, Ramezanzadeh B, Dehghani A, Ramezanzadeh M. Novel cost-effective and high-performance green inhibitor based on aqueous *Peganum harmala* seed extract for mild steel corrosion in HCl solution: detailed experimental and electronic/atomic level computational explorations. Journal of Molecular Liquids. 2019;283:174-95.
52. Bahrami MJ, Hosseini SMA, Pilvar P. Experimental and theoretical investigation of organic compounds as corrosion inhibitor for mild steel corrosion in sulphuric acid medium. Corrosion Science. 2010;52:2793-2803.
53. Padash R, Rahimi-Nasrabadi M, Shokuhi Rad A, Sobhani-Nasab A, Jesionowski T, Ehrlich H. A theoretical study of two novel Schiff bases as inhibitors of carbon steel corrosion in acidic medium. Applied Physics A. 2019;125(78):1-11.

54. Zhanga J, Lia W, Zuob X, Chenc Y, Luoa W, Zhanga Y, *et al*. Combining experiment and theory researches to insight into anticorrosion nature of a novel thiazole derivative. Journal of the Taiwan Institute of Chemical Engineers. 2021;122:190-200.
55. Issaadi S, Douadi T, Chafaa S. Adsorption and inhibitive properties of a new heterocyclic furan Schiff base on corrosion of copper in HCl-1M: Experimental and theoretical investigation. Applied Surface Science, 2014, 582-589.
56. Verma CB, *et al*. A thermodynamical, electrochemical, theoretical and surface investigation of diheteroaryl thioethers as effective corrosion inhibitors for mild steel in 1 M-HCl. Journal of the Taiwan Institute of Chemical Engineers. 2016;58:127-140.
57. Parr RG, Szentpaly LV, Liu S. Electrophilicity index, Journal of the American Chemical Society. 1999;121:1922-1924.
58. Parr RG, Yang W. Density functional approach to the frontier-electron theory of chemical reactivity. Journal of the American Chemical Society. 1984;104(14):4049-4050.